

# Coherent Interactions in Nucleus-Nucleus Collisions

Joakim Nystrand

*Div. of Cosmic and Subatomic Physics  
Department of Physics, Lund University  
Lund, Sweden*

*Presented at the IX<sup>th</sup> Blois Workshop on Elastic and Diffractive Scattering,  
Pruhonice near Prague, Czech Republic, June 9 – 15, 2001.*

## Abstract

At the Relativistic Heavy-Ion Collider (RHIC) at Brookhaven National Laboratory and at the Large Hadron Collider (LHC) at CERN, particles will be produced in coherent and diffractive nuclear interactions. In extremely peripheral nuclear collisions ( $b > 2R$ ), coherent interactions occur at very high rates and are dominated by photon-Pomeron or photon-meson processes. In these reactions, the photon and the Pomeron/meson from the electromagnetic and nuclear fields couple coherently to all nucleons. The rates for photonuclear interactions are roughly two orders of magnitude larger than for two-photon interactions at comparable center-of-mass energies.

## 1 Introduction

Ultra-relativistic nucleus-nucleus collisions are usually associated with copious particle production and complete disintegration of the projectile and target nucleus[1]. For very high center-of-mass energies, a new class of events can be distinguished, however, in which particles are produced in very peripheral collisions with no or very little disruption of the projectile and target. In these interactions, particles are produced through an interaction of the electromagnetic or nuclear fields of the ions. If the momentum transfers are small enough ( $Q < 1/R$ ), the fields couple coherently to all nucleons, which

has the effect of dramatically increasing the cross sections. The coherence requirement also gives the events a distinct transverse momentum distribution, which can be used to identify the events, as will be discussed below.

Coherent electromagnetic interactions can happen for impact parameters of 10's or 100's of fermi because of the long range of the electromagnetic field. The leptodermous nature of ordinary nuclei, together with their finite spatial extent of a few fermi, thus ensures that these interactions can be clearly separated from hadronic interactions in impact parameter space.

The Relativistic Heavy-Ion Collider (RHIC) at Brookhaven National Laboratory is the first heavy-ion accelerator energetic enough for significant production of hadronic final states in coherent nuclear interactions. The first collisions at RHIC were achieved in the summer last year, and the STAR collaboration has already shown the feasibility of experimentally studying these interactions[2]. The Large Hadron Collider at CERN, when it is operated with heavy-ions, will also produce coherent interactions with large cross sections.

In this talk, I will give an overview of two-photon and coherent photonuclear interactions in nucleus-nucleus collisions at RHIC and the LHC.

## 2 The method of equivalent photons

The Lorentz contracted electromagnetic fields of a relativistic heavy ion can be treated as a stream of equivalent photons. This is the so-called Weizsäcker-Williams method[3]. In the impact parameter representation, the density of photons at a perpendicular distance  $b$  ( $b > R$ ) from the center of the ion is

$$n(\omega, b) = \frac{dN_\gamma}{d\omega d^2b} = \frac{\alpha Z^2}{\pi^2} \frac{1}{\omega b^2} x^2 K_1^2(x) . \quad (1)$$

where  $\omega$  is the photon energy and  $x = b\omega/\gamma$ ,  $\alpha$  is the fine structure constant, and  $K_1(x)$  is the modified Bessel function[4]. Natural units, in which  $\hbar = c = 1$ , are used. Note that the density of photons is proportional to  $Z^2$ .

The photons from one of the nuclei may interact coherently with the electromagnetic or nuclear field of the other nucleus. In the latter case, the interactions is of the type photon-meson or photon-Pomeron, whereas a purely electromagnetic interaction is referred to as a two-photon interaction, although higher-order processes are also possible.

The total number of equivalent photons of a given energy is obtained by integrating Eq. 1 over all impact parameters with a suitable minimum impact parameter cut-off. For a single nucleus, this cut-off is usually given by the nuclear radius,  $R$ . The full photon spectrum in a heavy-ion interaction is

Accelerator	Ion	A	Z	$E_{BEAM}$ [A GeV]	$\gamma$	Luminosity
RHIC	Au	197	79	100	108.4	$2 \cdot 10^{26} \text{ cm}^{-2} \text{ s}^{-1}$
LHC	Pb	208	82	2,760	2940	$4 \cdot 10^{26} \text{ cm}^{-2} \text{ s}^{-1}$

Table 1: Some data for the heaviest beam nuclei at RHIC and LHC.

not useable, however, since for impact parameters  $b < 2R$  hadronic interactions dominate and it is generally not possible to distinguish electromagnetic interactions. The spectrum for two colliding nuclei can then be calculated from[5]

$$n(\omega) = \frac{dN_\gamma}{d\omega} = \int_0^\infty 2\pi b db [1 - P_{Had}(b)] \int_0^R \frac{r dr}{\pi R^2} \int_0^{2\pi} d\varphi n(\omega, b + r \cos(\varphi)) \quad (2)$$

Here,  $P_{Had}$  is the probability of having a hadronic interaction at impact parameter  $b$ .  $P_{Had}$  is calculated using a Glauber model with the total nucleon-nucleon cross section as input. The integrals over  $R$  and  $\varphi$  correspond to an averaging of the flux over the transverse surface of the nucleus.

The total production cross section can be calculated as the convolution of the photon spectrum with the  $\gamma A$  photonuclear cross section:

$$\sigma(A + A \rightarrow A + A + X) = \int n(\omega) \sigma_{\gamma A}(\omega) d\omega. \quad (3)$$

The photonuclear cross section for the photon-Pomeron/meson and two-photon production mechanisms will be discussed in the next two sections.

### 3 Vector meson production

A photon might interact hadronically by fluctuating into a virtual quark anti-quark pair. The  $q\bar{q}$ -pair prefer to act as a vector meson to conserve the spin of the photon. According to the so-called Vector Meson Dominance Model[6], the scattering amplitude for photon-hadron interactions factorizes into a product of the probability for the fluctuation into the vector meson state and a hadronic cross section:

$$\frac{d\sigma}{dt}(\gamma A) = \sum_V \frac{4\pi\alpha}{f_V^2} \frac{d\sigma}{dt}(VA), \quad (4)$$

where  $f_v$  is the photon vector meson coupling, and  $\sqrt{t}$  is the momentum transfer from the target nucleus, summed over the vector meson states. Neglecting cross terms (i.e. cases where the photon fluctuates into a state  $V$

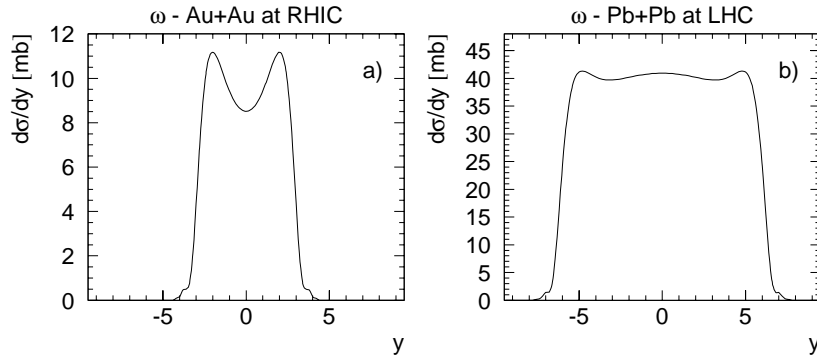


Figure 1: Rapidity distributions of  $\omega$ -mesons at RHIC and LHC.

and then scatters off the target into a state  $V'$ ), the hadronic part of the interaction can thus be treated as elastic scattering. For elastic scattering, the photonuclear cross section can be written as a product of a constant forward scattering amplitude times an integral over  $t$  of the nuclear form factor squared,

$$\sigma_{\gamma A}(\omega) = \frac{d\sigma}{dt} \Big|_{t=0} \int_{t_{min}}^{\infty} |F(t)|^2 dt, \quad (5)$$

where  $\sqrt{t_{min}} = (M_V^2/2\omega)$  is the minimum momentum transfer needed to produce a vector meson with mass  $M_V$ . The forward scattering amplitude is related to the total cross section through the optical theorem

$$\frac{d\sigma(VA \rightarrow VA)}{dt} \Big|_{t=0} = \frac{\sigma_{tot}^2(VA)}{16\pi} \quad (6)$$

The nuclear forward scattering amplitude can be expressed in terms of the photon-nucleon cross section,  $\sigma(\gamma N)$ :

$$\frac{d\sigma(\gamma A \rightarrow VA)}{dt} \Big|_{t=0} = \left( \frac{\sigma_{tot}(VA)}{\sigma_{tot}(VN)} \right)^2 \frac{d\sigma(\gamma N \rightarrow VN)}{dt} \Big|_{t=0}. \quad (7)$$

Measurements of coherent photonuclear vector meson production can provide information on the total vector meson nucleus cross section, and hence on the mean free path of vector mesons in nuclear matter. In ref. [5], data on  $\gamma N \rightarrow VN$  from HERA and fixed target experiments were used as input to determine  $\sigma_{tot}(VN)$ . This was then used to calculate  $\sigma(VA)$  and  $\sigma(\gamma A)$  from a Glauber model. The corresponding nucleus-nucleus cross sections were calculated using the photon spectrum of Eq. 2. The cross sections for

vector meson production at RHIC and the LHC (Table 2) were found to be very large, roughly 10% of the total inelastic hadronic Au+Au cross section at RHIC, rising to 50% for Pb+Pb collisions at the LHC.

The vector mesons are produced near mid-rapidity. As an example, the rapidity distributions of  $\omega$ -mesons at RHIC and LHC are shown in Fig. 1.

	$\rho^0$	$\omega$	$\phi$	$J/\Psi$
RHIC Au+Au	590	59	39	0.29
LHC Pb+Pb	5200	490	460	32

Table 2: Vector meson production cross section [mb] with heavy ions at RHIC and the LHC, from [5].

## 4 Two-photon interactions

The cross section for meson production through the two-photon channel in  $\gamma A \rightarrow X A$  interactions is

$$\sigma_{\gamma A}(\omega) = 8\alpha Z^2 \frac{\Gamma_{\gamma\gamma}}{M_x^3} \int \left(\frac{\omega}{Q}\right)^4 |F(Q^2)|^2 \sin^2(\theta) d\Omega, \quad (8)$$

where  $\Gamma_{\gamma\gamma}$  and  $M_x$  are the two-photon width and mass of the meson,  $\theta$  is the scattering angle, and  $Q$  the momentum transfer[7]. With a simplified ansatz for the form factor,  $F(Q^2) = 1$  if  $Q < 1/R$  and 0 otherwise, the cross section becomes

$$\sigma_{\gamma A}(\omega) = 16\pi\alpha Z^2 \frac{\Gamma_{\gamma\gamma}}{M_x^3} \ln\left(\frac{2\omega}{M_x^2 R}\right) \quad (9)$$

The cross section thus increases logarithmically with the photon energy. Using a more realistic form factor

$$F(Q^2) = \frac{3}{(QR)^3} \left[ \sin(QR) - QR \cos(QR) \right] \left[ \frac{1}{1 + a^2 Q^2} \right], \quad (10)$$

where  $a=0.7$  fm reflects the nuclear skin thickness, the cross section for two-photon production of  $\eta$ -mesons is compared with the photonuclear cross section for  $\omega$ -mesons (Eq. 5) in Fig. 2.

The cross section for two-photon production is between one and two orders of magnitude smaller than that for photonuclear production up to photon energies of  $10^4$  GeV. The energy dependence is very different for the two

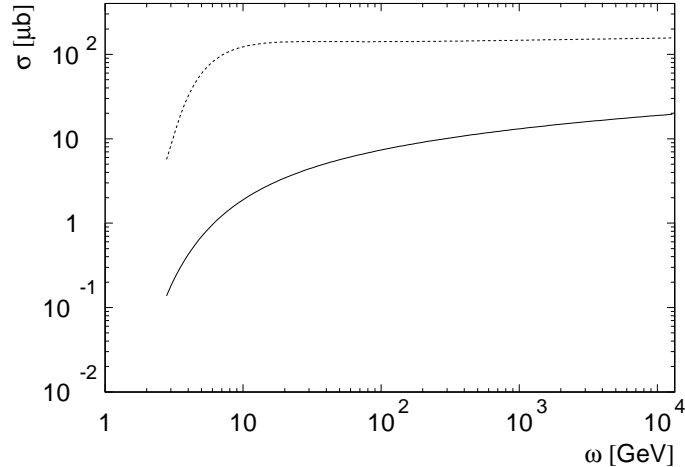


Figure 2: Cross sections for coherent photonuclear production of  $\omega$ -mesons (dotted curve) and two-photon production of  $\eta$ -mesons (solid curve) in  $\gamma$ +Cu interactions as functions of the photon energy,  $\omega$ , in the nuclear rest frame.

production mechanisms. The photonuclear cross section is essentially independent of energy above threshold, whereas the two-photon cross section increases logarithmically with  $\omega$ .

In heavy-ion interactions it is necessary to exclude interactions where the nuclei overlap to obtain realistic cross sections for two-photon processes[8]. The differential cross section is given by

$$\frac{d\sigma}{dW dy} = \frac{W}{2} \int_{b_1 > R} \int_{b_2 > R} n(\omega_1, b_1) n(\omega_2, b_2) \sigma_{\gamma\gamma} \Theta(|\vec{b}_1 - \vec{b}_2| - 2R) d^2\vec{b}_1 d^2\vec{b}_2, \quad (11)$$

where  $Y$  and  $W$  are the rapidity and center of mass energy of produced state. The  $\Theta$ -function removes the contribution from interactions with overlap.

## 5 Interference and transverse momentum

It is generally not possible to tag the outgoing nuclei in a coherent interaction. The coherence requirement limits the transverse momentum transfers to about  $\Delta p_T < \hbar c/R$ . This means that the angular deflection of the ions will be of the order of

$$\theta \sim \frac{0.175}{\gamma \cdot A^{4/3}} \quad (12)$$

This is a few  $\mu\text{rad}$  at RHIC and a few tenths of a  $\mu\text{rad}$  at LHC.

Experimental identification of coherent events can instead be achieved through the transverse momentum obtained by reconstructing all particles emitted in the event[2, 9].

The transverse momentum distribution of virtual photons of energy  $\omega$  is given by[10]

$$\frac{dN_\gamma}{dk_\perp} \propto \frac{|F((\omega/\gamma)^2 + k_\perp^2)|^2}{((\omega/\gamma)^2 + k_\perp^2)^2} k_\perp^3. \quad (13)$$

Similarly, the distribution of the nuclear transverse momentum transfer,  $q_\perp$ , is given by the form factor[11]

$$\frac{dN_P}{dq_\perp} \propto |F(t_{min} + q_\perp^2)|^2 q_\perp. \quad (14)$$

The transverse momentum distribution of the produced state is given by the convolution of the transverse momentum distributions of the two sources

$$\frac{dn}{dp_T} = \int f_1(\vec{p}_T) f_2(\vec{p}_T - \vec{p}_T) d^2\vec{p}_T. \quad (15)$$

The  $p_T$  distribution for states produced in two-photon interactions at midrapidity is shown in Fig. 3. The shape of the distribution depends on the mass of the final state. The corresponding distribution for photonuclear production of  $\phi$  and  $J/\Psi$  mesons are shown as the dashed curve in Fig. 4. The photonuclear  $p_T$  distributions are dominated by the nuclear form factors and are much less sensitive to the mass of the produced state.

The situation for photonuclear production is, however, a little bit more complicated. Consider the differential cross section for the production

$$\frac{d\sigma}{dydp_T} = \int \omega_1 \frac{dN}{d\omega_1 d^2b} \sigma(\gamma A_2) f_{1,2}(p_T) + \omega_2 \frac{dN}{d\omega_2 d^2b} \sigma(\gamma A_1) f_{2,1}(p_T) d^2b, \quad (16)$$

where the two terms correspond to production off each of the two nuclei.

Adding the cross section is only valid as long as  $p_T \ll 1/b$ , however, since for smaller transverse momenta, the two sources will be indistinguishable, and one then has to add the amplitudes[11]. At midrapidity, where the contributions from the two sources are of equal magnitude, and if one assumes that the outgoing vector mesons can be treated as plane waves, the integral over  $b$  in Eq. 16 becomes

$$\frac{d\sigma}{dydp_T} = \int |A_1 + A_2|^2 d^2\vec{b} = 2 \int |A_1|^2 (1 - \cos(\vec{p}_T \cdot \vec{b})) d^2\vec{b}. \quad (17)$$

Here,  $A_1$  and  $A_2$  are the amplitudes for production off nucleus 1 and 2, respectively. This has the effect of modifying the transverse momentum

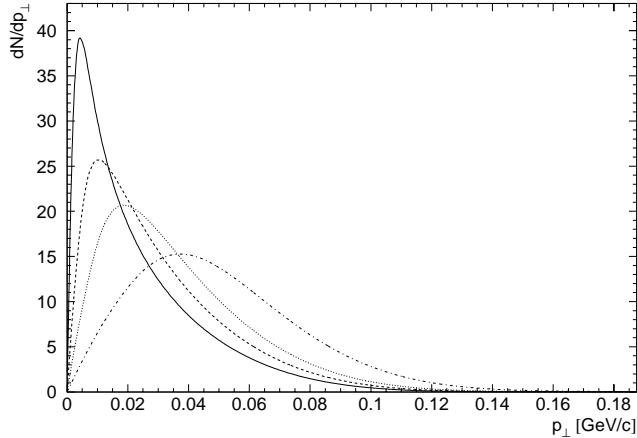


Figure 3: Transverse momentum spectra for two-photon states at midrapidity for  $\gamma\gamma$  center-of-mass energies of 0.2 (solid), 0.5 (dashed), 1.0 (dotted), and 3.0 (dash-dotted) GeV in Au+Au interactions at RHIC.

spectrum to that shown by the solid curve in Fig. 4. The interference pattern is essentially that of a two-source interferometer.

This interference is of particular interest since the  $c\tau$  of the vector mesons (except for the  $J/\Psi$ ) are generally much shorter than the median impact parameters in the interactions. A vector meson produced at one nucleus will thus have decayed before information of its production have reached the other nucleus. For interference, the decay particles must thus be in an entangled state and retain information about their origin long after the decay occurred.

## 6 Strong fields and multiple excitations

Because of the strong fields associated with ultra-relativistic heavy-ions, the probabilities for several electromagnetic processes are very large at small impact parameters, and calculated, un-unitarized first-order probabilities may even exceed 1 [12]. This is for example the case for two-photon production of  $e^+e^-$  pairs.

Another process with very high interaction probability is mutual Coulomb dissociation. The dominating process is photonuclear excitation of the target into a Giant Dipole Resonance followed by emission of one or more neutrons[13]. The probability for mutual Coulomb dissociation reaches about 35% in a grazing Au+Au collision at RHIC.

Coherent vector meson production can occur in coincidence with Coulomb



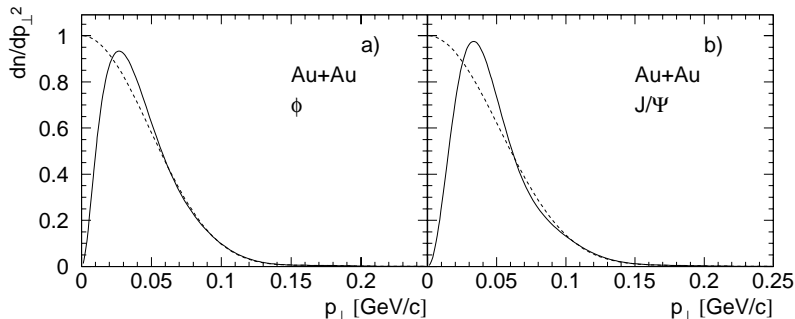


Figure 4: Transverse momentum spectra with (solid) and without (dashed) interference for  $\phi$  and  $J/\Psi$  production in Au+Au collisions at RHIC.

excitation of one or both nuclei[2]. If one assumes that the Coulomb excitation and the vector meson production occur independently, the cross section can be calculated from

$$\sigma(A + A \rightarrow A^* + A^* + V) = \int (1 - P_{Had}(\vec{b})) P_{Coul}(\vec{b}) P_V(\vec{b}) d^2\vec{b} \quad (18)$$

where  $P_{Had}$ ,  $P_{Coul}$ , and  $P_V$  are the hadronic, Coulomb, and vector meson production probabilities, respectively.

Using the same formalism for vector meson production as in [5] and the Coulomb reaction probabilities calculated in [13], Eq. 18 gives cross sections of 42 mb for  $\rho^0$ , 4 mb for  $\omega$ , 3 mb for  $\phi$ , and 0.29 mb for  $J/\Psi$  production in Au+Au interactions at RHIC. The cross sections are reduced by roughly a factor of 10 compared with no breakup.

Requiring production in coincidence with nuclear breakup also reduces the median impact parameters in the interactions by about a factor of 2. This should affect the interference discussed above.

## 7 Conclusions

Electromagnetic interactions will occur with high rates in peripheral nucleus-nucleus collisions at RHIC and LHC. The two-photon and coherent photonuclear production mechanisms have been discussed and compared. New phenomena, such as multiple excitations in strong fields and interference, not accessible in similar reaction channels in  $e^+e^-$  and  $eA$  interactions, can be studied with heavy ions.

## Acknowledgements

I would like to acknowledge Spencer Klein, LBNL, Berkeley, my collaborator in the studies of vector mesons and interference. I would like to thank Tony Baltz and Sebastian White, BNL, Brookhaven, for providing the Coulomb interaction probabilities from their paper[13] and for useful discussion. This project was supported by the Swedish Research Council (VR).

## References

- [1] For a review see Proc. XIV International Conference on Ultra-relativistic Nucleus- Nucleus collisions (Quark Matter 99), Torino, Italy, May 10 - 15, 1999, Nucl. Phys. **A661** (1999); and proceedings from previous Quark Matter conferences.
- [2] J. Seger for the STAR Collaboration, these proceedings.
- [3] E. Fermi Z. Phys. **29**, 315 (1924); E.J. Williams Proc. Roy. Society London **A 139**, 163 (1933); Kgl. Danske Videnskap. Mat.-fys. Medd. **13**, No. 4 (1935); C. Weizsäcker Z. Phys. **88**, 612 (1934).
- [4] J.D. Jackson *Classical Electrodynamics* 2nd Ed., John Wiley & Sons, New York (1975), Eq. 15.52.
- [5] S.R. Klein and J. Nystrand Phys. Rev. **C 60**, 014903 (1999).
- [6] A. Donnachie and G. Shaw, in *Electromagnetic Interactions of Hadrons*, Eds. A. Donnachie and G. Shaw (Plenum Press, 1978), Vol. 2, p. 169.
- [7] V.M. Budnev et al., Phys. Rep. **15C**, 181 (1975).
- [8] R.N. Cahn and J.D. Jackson, Phys. Rev. **D 42** 3690 (1990); G. Baur and L.G. Ferreira Filho, Nucl. Phys. **A 518**, 786 (1990);
- [9] J. Nystrand and S.R. Klein, in Proc. Workshop on Photon Interactions and the Photon Structure, Lund, Sweden, Sept. 10-13, 1998, nucl-ex/9811007.
- [10] M. Grabiak, B. Müller, W. Greiner, G. Soff, P. Koch J. Phys. **G 15**, L25 (1989); M. Vidovic, M. Greiner, C. Best, G. Soff Phys. Rev. **C 47**, 2308 (1993).
- [11] S.R. Klein and J. Nystrand Phys. Rev. Lett. **84**, 2330 (2000).
- [12] C.A. Bertulani and G. Baur, Phys. Rep. **163**, 299 (1988).
- [13] A.J. Baltz, C. Chasman, S.N. White Nucl. Inst. Meth. **417**, 1 (1998).